Advances in Computational & Experimental Engineering & Science

Analysis of Large Deflection Problems of Beams Using a Meshless Local Petrov-Galerkin Method

I. S. Raju[1]

Summary

The Meshless Local Petrov-Galerkin (MLPG) method that uses radial basis functions, MLPG (RPG) in the development of trial functions, is applied to two nonlinear beam-bending problems – the Elastica and the large deflections of a cantilever beam with a tip load. The present MLPG (RPG) method is formulated with an iterative procedure to account for the nonlinearity. The present method yields very accurate solutions for the problems considered.

Introduction

Meshless Galerkin and Petrov-Galerkin formulations were presented for beam (C^1) problems using generalized moving least squares (MLS) interpolants in references 1 and 2. An alternative MLPG (RPG) method with radial basis functions (RBF) that is as accurate as the MLPG method is presented in reference 3. In this paper, the RPG method is applied to two nonlinear beam-bending problems to evaluate its effectiveness.

Analysis

The Euler-Bernoulli equation of bending for an initially straight beam (Fig. 1) is [4]

$$\frac{d\theta}{ds} = \frac{(d^2w/dx^2)}{[1+(dw/dx)^2]^{3/2}} = -\frac{M}{EI}, \tag{1}$$

where $M=M(x)$ is the bending moment, w is the deflection, θ is the slope, and EI is the flexural rigidity of the beam. In most engineering problems, (dw/dx) is small and its square is small compared to unity and hence θ=(dw/dx). Eq. (1) then reduces to

$$EI(d^2w/dx^2) = -M\ . \tag{2}$$

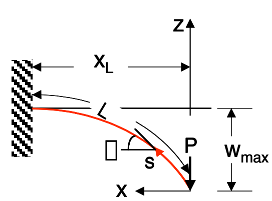

Figure 1: Large deflections of a cantilever beam

[1] NASA Engineering and Safety Center, NASA Langley Research Center, Hampton, Virginia, 23681-2199, USA

Proceedings of the 2004 International Conference on Computational & Experimental Engineering & Science 26-29 July, 2004, Madeira, Portugal

Equation (2) can be easily solved for various loading conditions. When the slope (dw/dx) is not small in comparison to unity then the moment $\square$ itself is a nonlinear function of $\square$ and the problem is difficult to analyze in terms of w and x. Instead, the problem becomes tractable in terms of $\square$ and M [5,6]. Differentiating Eq. (1) with respect to s, one obtains

$$EI(d^2\square/ds^2) = \square(dM/ds) = \square V\ , \tag{3}$$

where V is the shear force. With Eq. (3) as the starting point, the Elastica and the nonlinear bending of a cantilever beam are analyzed using the MLPG (RPG) method.

The Elastica

Consider a column as shown in Figure 2. When the magnitude of the load P is higher than the Euler buckling load of the column, large deflections would occur and the governing equation can be written using Eq. (3) as

$$d^2\square/ds^2 = \square(P/EI)\sin(\square)\ , \tag{4}$$

subjected to the boundary conditions $\square$=0 at s=L and ($d\square/ds$)=0 at s=0. Using a non-dimensional coordinate $\square$=(s/L), Eq. (4) can be written as

$$d^2\square/d\square^2 + \square\sin(\square) = 0\ , \tag{5}$$

where $\square=PL^2/EI$. Eq. (5) represents a nonlinear problem because of the sin($\square$) term. An MLPG solution of Eq. (5) will be attempted by developing the weak form as

$$\square_{\square}[d^2\square/d\square^2 + \square\sin(\square)]\cdot v\cdot d\square = 0\ , \tag{6}$$

where $\square$ is the domain under consideration ($0\square\square\square 1$), and v is a weighting function. The weak form is rewritten using a linearizing function f :

$$\square_{\square}[d^2\square/d\square^2 + \square\cdot\square\cdot f\,]\cdot v\cdot d\square = 0,\ \text{where } f = \sin(\square)/\square. \tag{7}$$

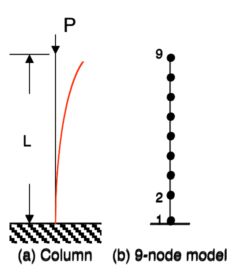

Figure 2: A column and the 9-node model

Equation (7) is integrated by parts to set up the weak form (see references 1- 3),

$$\square \int_{\square} (d\square / d\square)\cdot(dv/d\square)d\square + [(d\square/d\square)\cdot v]_{\square I} + \int_{\square} \square\cdot\square\cdot f\cdot v\, d\square = 0\,. \tag{8}$$

Next, the trial and test functions are assumed for □and *v*, respectively. The trial functions for □ are assumed as

$$\square = \sum_{j=1}^{N} \square_j(\square)\cdot\square_j\,, \tag{9}$$

where $\square_j(\square)$ is the shape function and $\square_j$ is the value of the slope at node *j* of an *N*-node meshless model [1-3]. The shape functions $\square_j(\square)$ are derived from the RBF

$$t_j = \left|(x \square x_j)\right| = \left|(\square - \square_j)\right|\,. \tag{10}$$

Details of the development of the shape functions from the assumed RBF follow similar procedures presented in reference 3. Next, the test functions v_i are chosen so that v_i and $(dv/d\square)_i$ are zero at the ends of the domain $\square_{\square}$ as in reference 2. In this implementation, the test functions with □=4 in Eq. 34 of reference 2 are used.

The trial and test functions are substituted into Eq. (8) to yield

$$\sum_{j=1}^{N} [\square \int_{\square S_i} \frac{d\square_j}{d\square}\cdot\frac{dv_i}{d\square}\cdot d\square + (\frac{d\square}{d\square}\cdot v_i)_{\square I} + \int_{\square S_i} \square\cdot\square_j\cdot f\cdot v_i\, d\square]\square_j = 0\,, \tag{12}$$

where *i=1,2…N*. Note that the term $[(d\square/d\square)\cdot v_i]$ evaluated on $\square_{\square}$ is identically zero as v_i is zero on $\square_{\square}$ and hence drops out of Eq. (12). For an *N*-node model, Eq. (12) can be written as

$$[K]\{d\} + \square\cdot[K_G]\{d\} = \{0\}\,, \tag{13}$$

where $[K]$ and $[K_G]$ are NxN matrices formed using $[k]$ and $[k_G]$ as

$$k_{ij} = \int_{\square s_i} (d\square_j/d\square)\cdot(dv_i/d\square)d\square,\quad k_{G\,ij} = \int_{\square s_i} \square_j\cdot f\cdot v_i d\square \quad \text{and} \tag{14}$$

$$\{d\} = \{\square_1, \square_2, \ldots\ldots \square_N\}^T\,. \tag{15}$$

The integrations involved in Eq. (14) are carried out numerically.

In the current implementation for the Elastica problem, the slope at the free end □ (i.e., value of □ at *s*=0) is assumed to be known. For each given value of □, the non-dimensional critical load λ is determined. To start the iteration, the deflection curve is assumed to be linear, i.e.,

$$\theta_j = (x_j / L) \cdot \alpha . \tag{16}$$

Utilizing these values of the slope, the function value of f ($f = sin(\theta)/\theta$) is evaluated at the Gaussian points and the $[K_G]$ matrix is developed. The eigenvalue problem in Eq. (13) is then solved to obtain λ. The corresponding eigenvector $\{d\}$ in terms of θ_j yields the values of θ_j for the next iteration. The iterative process is continued until the norm,

$$\|L_2\| = \sqrt{\frac{1}{N}\sum_{j=1}^{N}[\theta_j^{(q+1)} - \theta_j^{(q)}]^2} , \tag{17}$$

for successive iterations q and $q+1$ is less than a prescribed tolerance. In this paper, a tolerance of 10^{-10} is used. The final values of the projected length and the maximum deflection of the column can be evaluated using [5,6]

$$(x_L / L) = \int_0^1 \cos(\theta) d\xi \quad \text{and} \quad (w_{\max} / L) = \int_0^1 \sin(\theta) d\xi . \tag{18}$$

In equations (18), the slope θ can be evaluated using the interpolation in Eq. (9). At the end of each iteration, the values of θ_j are known, and hence (x_L/L) and $(w_{\max}/L)$ can be calculated by numerically integrating Eq. (19).

Large Deflections of a Cantilever Beam

Next, the large deflections of a cantilver beam subjected to a concentrated load at the free end (Fig. 1) are considered. The governing equation can be written using Eq. (3) as

$$d^2\theta / ds^2 = -(P / EI)\cos(\theta) , \tag{19}$$

subjected to the boundary conditions $\theta = 0$ at $s = L$ and $(d\theta/ds) = 0$ at $s = 0$. The weak form of Eq. (19) can be set up as

$$-\int_\Omega \frac{d\theta}{d\xi}\cdot\frac{dv}{d\xi} d\xi + (\frac{d\theta}{d\xi}\cdot v)_{\Gamma_I} + \int_\Omega \{-\frac{PL^2}{EI}\cos(\theta)\}\cdot v \cdot d\xi = 0 . \tag{20}$$

Assuming trial and test functions for θ as in Eq. (9) and v as previously mentioned leads to

$$[K]\{d\} = \{F\} , \tag{21}$$

where [K] is a NxN matrix formed by using k_{ij} in Eq. (14) and

$$F_i = \int_{\square_{s_i}} (\square PL^2 / EI)\cos(\square)\cdot v_i d\square . \tag{22}$$

The integrations involved in Eq. (22) are performed numerically, and cos(□) is evaluated at the Gaussian point using the trial functions interpolation of Eq. (9).

Results and Discussion

The results for the Elastica are presented first. The large deflections of a cantilever beam with a concentrated tip load are discussed next. The results obtained with the present MLPG (RPG) method are compared to the exact solutions from the literature.

The Elastica: The column is idealized by several meshless models; 3-, 5-, 9-, 17-, and 33-node models. These models have equal nodal spacing ($\square x/L$). A typical 9-node model is shown in Figure 2. The $\square_{Si}$ is chosen to be ($2\square x/L$). Table 1 presents the convergence of the MLPG solution with model refinement for a large value of □, □=120º. This value of □ is chosen to demonstrate the effectiveness of the current MLPG solution. About 9 iterations are required for convergence for all the models considered. The critical load for □=120º obtained with the 33-node model is about 1.2 percent above the exact value. The values of (P/P_{cr}), (x_L/L), and (w_{max}/L) values for various values of □ from 0º to 176º (not shown here) are in excellent agreement with the exact solution.

Table 1: Convergence of the MLPG (RPG) solution: The Elastica, □=120^0

Nodes	$\square_{CR}$ at □=0	□	$\square/\square_{CR}$	x_L/L	w_{max}/L	Iterations
3	2.531	4.516	1.784	0.211	0.792	9
5	2.509	4.645	1.851	0.141	0.803	9
9	2.499	4.687	1.876	0.127	0.803	10
17	2.493	4.693	1.882	0.124	0.803	9
33	2.491	4.693	1.884	0.123	0.803	9
Exact [7]	2.467	4.648	1.884	0.123	0.803	

Cantilever Beam: The large deflections of a cantilever beam with a concentrated tip load are modeled with 9-, 17-, and 33-node models. Figure 3 presents the (x_L/L) and (w_{max}/L) as a function of the non-dimensional load (PL^2/EI). The results obtained with the 17-node model are shown in this figure as symbols. Larger values of the non-dimensional loads require higher number of iterations suggesting that the nonlinearity is much more severe as the magnitude of the load increases. The exact solution for this problem is available (see references 5 and 6) in terms of elliptic integrals and is shown in this figure as a continuous curve. Excellent agreement is observed between the two sets of results suggesting that the present MLPG (RPG) gives accurate solutions to nonlinear beam-bending problems.

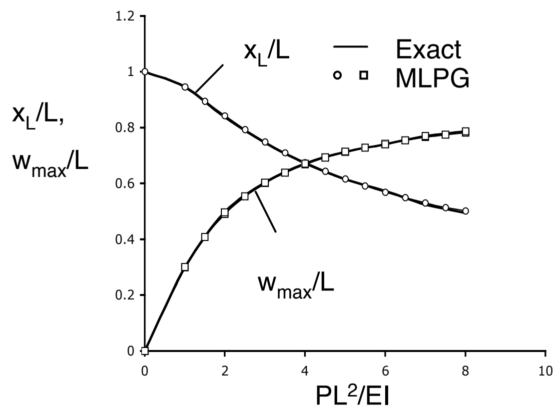

Fig. 3: Comparison of MLPG and the exact solutions of a cantilever beam shown in Fig.1

Concluding Remarks

The large deflections problems of buckled column (the Elastica) and large deflection of a cantilever beam with a concentrated tip load are considered. The weak form of the nonlinear governing differential equations is developed. A Meshless Local Petrov-Galerkin method is developed using the developed weak form. Radial basis functions are used to develop the trial functions of the primary variable, the slope of the deflection curve. An iterative procedure is developed to account for the nonlinearity in the problem. The results obtained by this method are compared to the exact solutions from the literature. The MLPG (RPG) method yields very accurate solutions.

References

1 Atluri, S. N., Cho, J. Y., and Kim, H. -G. (1999): "Analysis of thin beams, using the meshless local Petrov-Galerkin method, with generalized moving least squares interpolations," *Computational Mechanics*, Vol. 24, pp. 334-347.

2 Raju, I. S. and Phillips, D. R. (2003): "Further developments in the MLPG method for beam problems," *CMES: Computer Modeling in Engineering & Sciences*, Vol. 4, No. 1, pp. 141-159.

3 Raju, I. S., Phillips, D. R., and Krishnamurthy, T. (2003): "Meshless local Petrov-Galerkin Euler-Bernoulli beam problems: a radial basis function approach," Proceedings of the 44th SDM Conference, Norfolk, Virginia, April 7-10, 2003.

4 Timoshenko, S. P. (1986): *Strength of Materials*, Third Edition.

5 Barton, H. J., (1944): "On the deflections of a cantilever beam", *Quarterly of Applied Mathematics,* Vol. 2, pp. 168-171, and (1945) Vol. 3, pp. 275-276.

6 Bisshopp, K. E. and Drucker, D. C. (1945): "Large Deflection of cantilever beams", *Quarterly of Applied Mathematics*, Vol. 3, pp. 272-275.

7 Timoshenko, S. P. and Gere, J. M. (1963): *Theory of Elastic Stability*, McGraw Hill, Second Edition.